Mine Water and the Environment
https://doi.org/10.1007/s10230-020-00703-9

TECHNICAL ARTICLE

Impact of Mine Leachates on a Carbonate Aquifer (SE Spain)

M. A. Díaz-Puga[1] · A. Pulido-Bosch[2] · A. Vallejos[1] · F. Sola[1] · L. Daniele[3,4] · M. Simón[5] · I. García[5]

Received: 11 February 2020 / Accepted: 8 July 2020

Abstract
In October 1966, an intense precipitation event (190 mm in 24 h) broke an old tailings retaining structure in the "El Segundo" mining district in the western sector of Spain's Sierra de Gador, generating a contaminated flood. The Pb-F rich mixture flowed for more than 12 km through the dry riverbeds, damaging infrastructures and crops. In March, 2010, over 40 years later, 41 samples were collected from boreholes and springs, along with eight sediment samples from near the tailings pond and along the dry riverbeds. The fluoride levels in the area's groundwater were close to 1 ppm, surpassing the area's normal geogenic levels, and in some cases exceeding the WHO maximum recommended value for drinking water, despite the time that has elapsed since the event. Less mobile elements, such as Pb and Zn, also had higher concentrations in the area affected by the sludge contamination, but did not significantly exceed the background geogenic values.

Keywords Tailings dam failure · Fluorine · Groundwater pollution

Introduction

Mining is an economic activity associated with many environmental issues, but one of the greatest potential risks are tailings dam failures (Owen et al. 2020). When these events occur, tons of highly concentrated and potentially contaminant mud flood wide areas downstream. Much attention has been paid to the effects of tailings failures when the flows have been rich in metals (Hatje et al. 2017; Macías et al. 2015; Resongles et al. 2014; Queiroz et al. 2018; Thompson et al. 2020), but this is not the case for failures involving other elements, such us fluorine.

Fluorine is a relatively abundant element in nature, with an average concentration of 540 ppm in the continental crust. In natural waters, it mainly appears as free fluoride (F^-) ion, although it can form complexes with other elements in specific conditions (Gosselin et al. 1999). The concentration of F^- in water is highly variable, with values ranging from trace levels to tens of milligrams per liter (WHO 2017). In surface waters, such as rivers and lakes, fluorine concentrations are generally less than in groundwater, with values between 0.01 and 0.3 ppm (Murray 1986). However, there are exceptions to these values, such as in some alkaline lakes, where concentrations can reach 2800 ppm of fluorine (Apambire et al. 1997; Fantong et al. 2010).

Multiple factors influence the F content of water. These include the geological formations water must cross, the solubility of F-rich minerals, the chemical composition of the water and soil, the ion exchange capacity of aquifer materials (OH^- for F^-), temperature, pH, water–rock interaction time, and evaporation. In general, however, a key factor is a high proportion of F-rich minerals in weathered and fractured rock (Rukah and Alsokhny 2004; Jacks et al. 2005). The F concentrations of water can be high in arid and semiarid regions with high evaporation and low recharge rates, and prolonged groundwater-rock interaction time (Edmunds and Smedley 2005; Kim and Jeong 2005). Similarly, water temperature and pH affect the concentrations of this ion (Darrell and Everett 1977).

The ingestion of high F concentrations is considered dangerous to human health. Excessive fluoride can lead to

✉ A. Pulido-Bosch
apulido@ual.es

1 Water Resources and Environmental Geology, University of Almería, Almeria, Spain

2 Department of Geodynamics, University of Granada, Granada, Spain

3 Department of Geology, FCFM, University of Chile, Santiago, Chile

4 Andean Geothermal Center of Excellence (CEGA), Fondap-Conicyt, Santiago, Chile

5 Soil Science Department, University of Almería, Almeria, Spain

Published online: 29 July 2020

dental and skeletal fluorosis, a disease that can cause mottling of the teeth and calcification of ligaments (Fawell et al. 2006; Kowalski 1999). For this reason, it is recommended that F concentrations not surpass 1.5 ppm in potable waters (Vithanage and Bhattacharya 2015).

The present work studies the effects of a fluorite mine tailings dam failure on the carbonate aquifer of the western sector of Sierra de Gador, Almeria. Hydrogeochemical data and soil composition were used to define the source of the F in the groundwater. This paper briefly addresses the origin and current status of groundwater pollution.

Geological Setting

The Sierra de Gador mining district (in the province of Almeria) is comprised of several hundred mines and trial pits, primarily dedicated to the extraction of Pb − Zn ± F. This mineralization appears in stratabound carbonate-hosted Mississippi Valley-type (MVT) deposits. The study area is focused on the westernmost sector of this area, in the proximity of the town of Berja, which is home to what was the largest mine in the district, known as the "El Segundo" mine (Figs. 1, 2).

The materials that comprise the Sierra de Gador belong to the Internal Zone of the Betic Range of the Alpujarride Complex (Martín-Rojas et al. 2007). They are composed of two formations: a basal unit composed of Permo-Triassic phyllites and a superior carbonated unit dating from the Middle Triassic period. The carbonate sequence starts with a basal dolomite unit followed by well stratified limestones. Interlayered in the limestone sequence are four dolomitic bands where the ores are located (Martín et al. 1987) (Fig. 3).

Mining in Sierra de Gador dates back to the third century B.C., initiated by the Carthaginians and later continued by the Romans and Arabs. The area boasts a long history of prolific mining production, particularly for the extraction of Pb, Zn, Fe and, to a lower extent, F, Cu, Au, and Ag (IGME 2002). In the 19 and 20th centuries, the province of Almeria was known worldwide for its lead mining industry.

As of the twentieth century, F extraction began in Sierra de Gador, taking advantage of the existing mineral dumps from past mining activities. Later, fluorite was extracted from underground and open-pit mines (Fenoll 1987; IGME

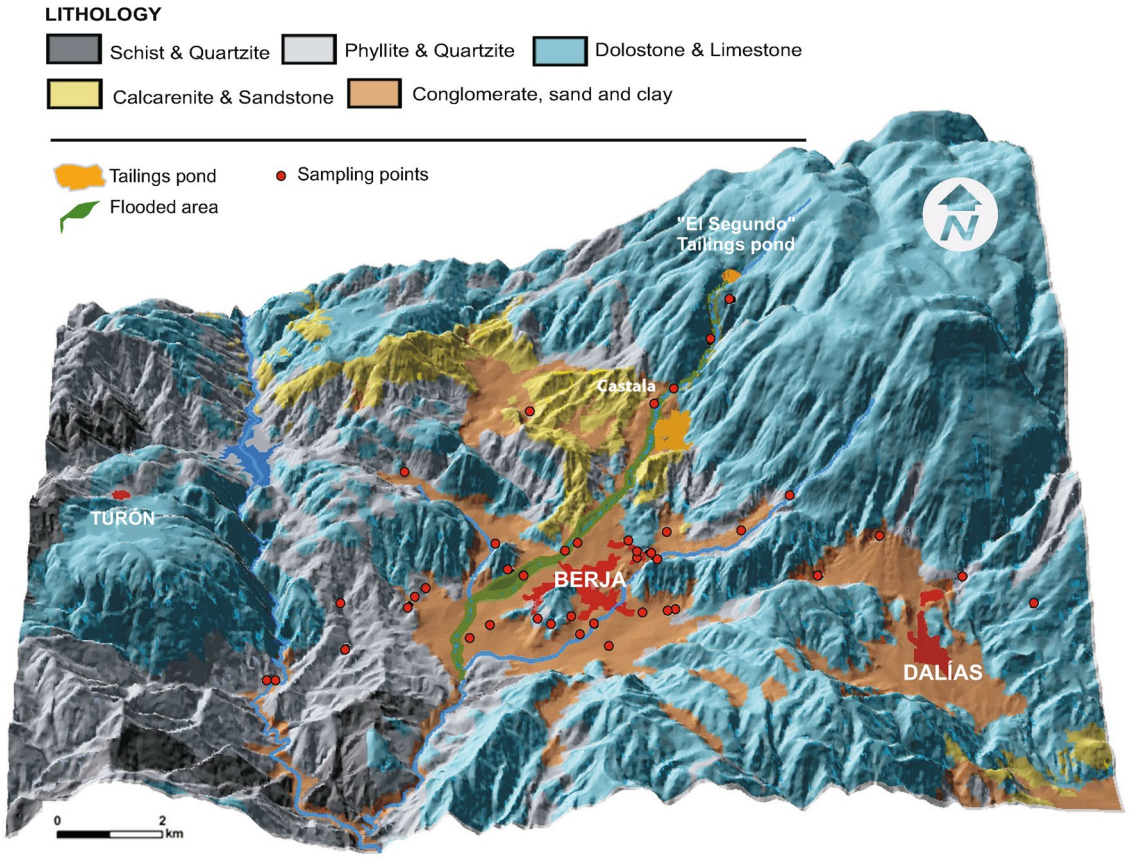

Fig. 1 3D geological map of the area affected by the tailings pond break in 1966

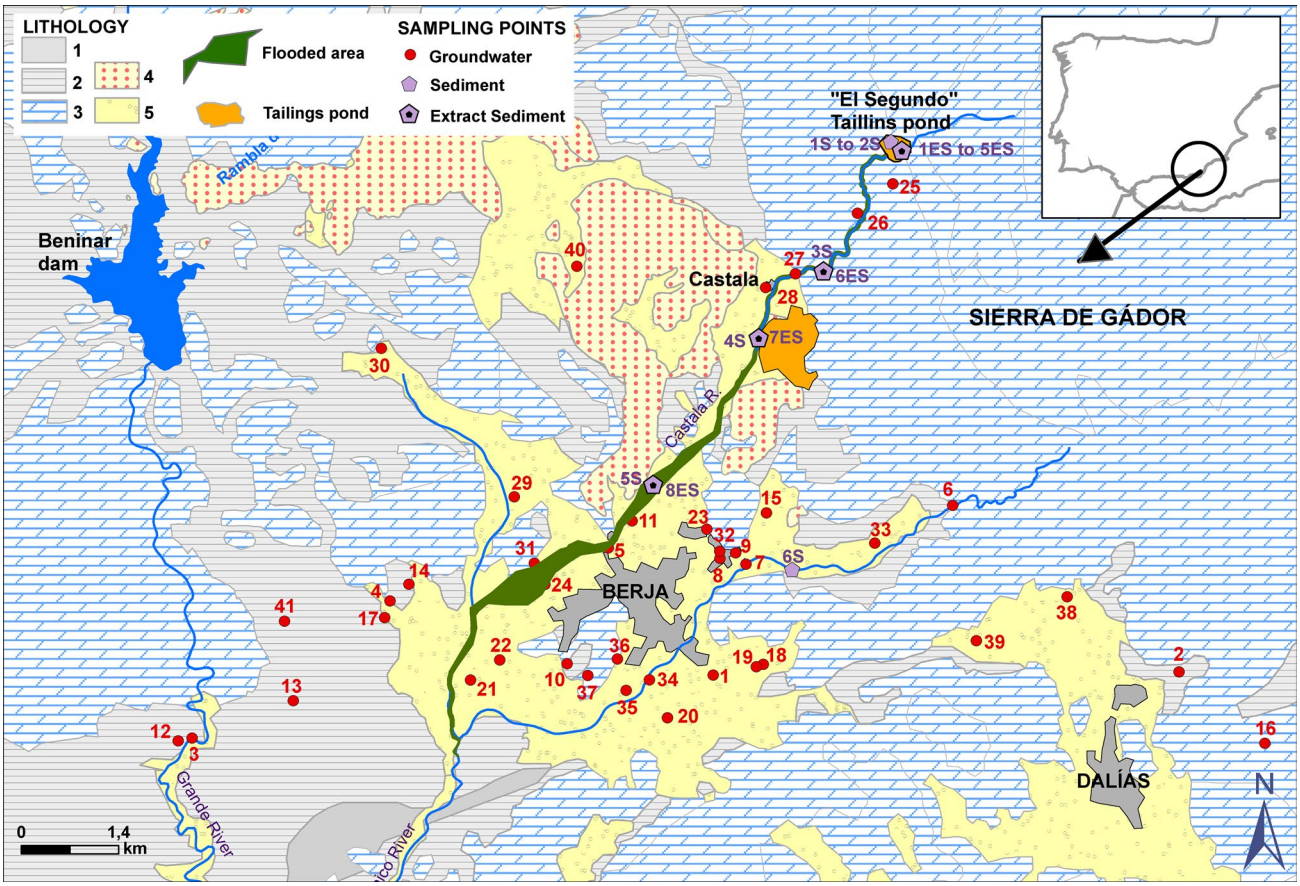

Fig. 2 Hydrogeological map of the study area showing the location of samples corresponding to groundwater, sediment and water extracts of the sediment. (1) Schist and quartzite, (2) phyllite and quartzite, (3) limestone and dolostone, (4) calcarenite, (5) conglomerate, sand and clay

2002). Mining for this mineral was concentrated in the western sector of Sierra de Gador.

The area known as "El Segundo" (in the town of Berja) was home to the largest mineral treatment plant (Pb and F; Fig. 1). The tailings were collected in a large pond adjacent to its facilities. In October 1966, the dam that contained the tailings pond broke due to heavy rainfall (190 mm in 24 h) and the instability of the masonry dam itself, flooding the surrounding area with contaminated mud (Fig. 4a). This sediment—mainly rich in F, Pb, and Zn—flowed along more than 12 km of the Castala river course, passing the town of Berja and causing damage to infrastructures and crops. The material was thus deposited in the areas bordering the dry riverbed. From this date, and due to this mining accident, all tailings was subsequently channeled via canals to the area of Castala, about 3 km NE of the town of Berja, where it was collected in a tailings pond covering more than 42 ha (Fig. 2). Today, most of that surface area continues to be covered by F-rich tailings, as are parts of the riverbed banks that were originally flooded (Fig. 4b). Consequently, this material still poses a risk of contaminating groundwater.

From a hydrogeological point of view, two different aquifers can be identified in the study area. The first consists of carbonates from the Alpujarride Complex, to which most of Sierra de Gador and its hills belong. The second aquifer, superjacent and connected to the first, is composed of detritic sediment. The latter is a relatively thin and small aquifer that occupies the Berja basin.

Materials and Methods

In March 2010, 41 groundwater samples were collected from boreholes and springs, along with eight soil samples (water extracts of soil) from the sludge of the tailings pond, as well as from the stream along which the flood flowed after the dam broke (Fig. 2). These samples were taken at depths between 0 and 20 cm at each point. Soil extracts were prepared at a soil–water ratio of 1:10 to determine pH, EC, and concentrations of the soluble fractions of the main components. The ionic concentrations were measured by means of an ICP-mass spectrometer at Acme Labs (Vancouver, Canada). In addition, six of the

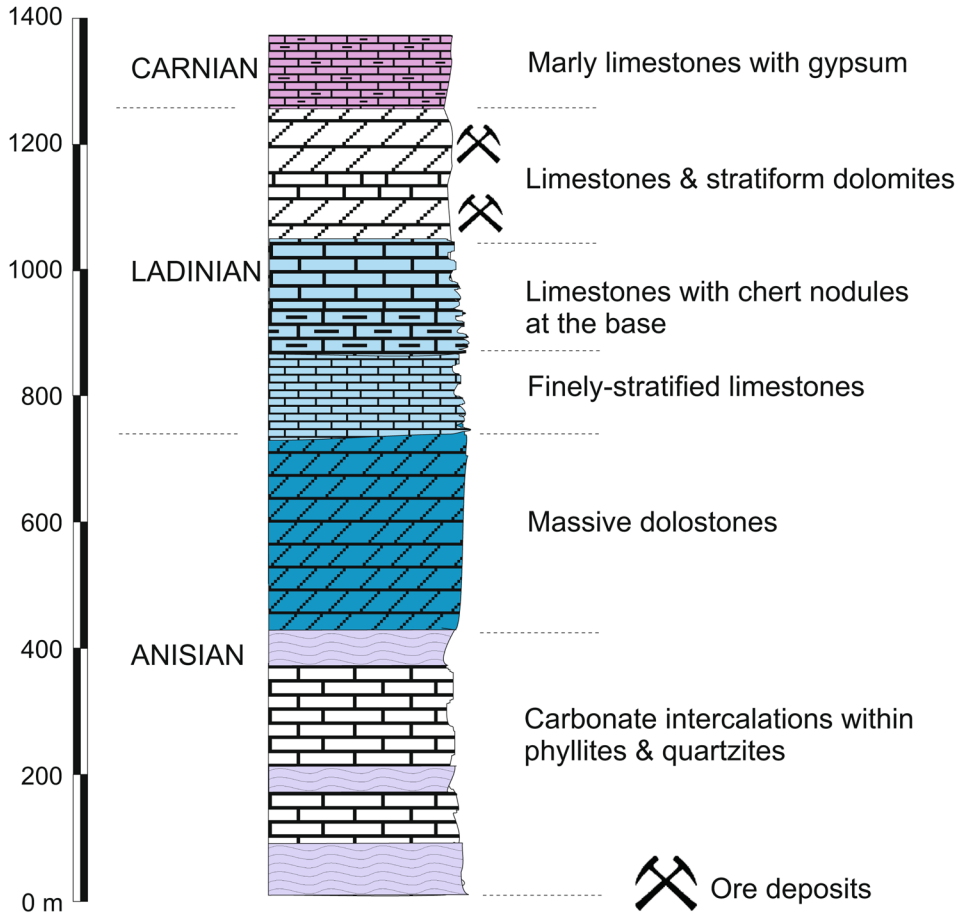

Fig. 3 General stratigraphic column (modified from Martin and Braga 1987)

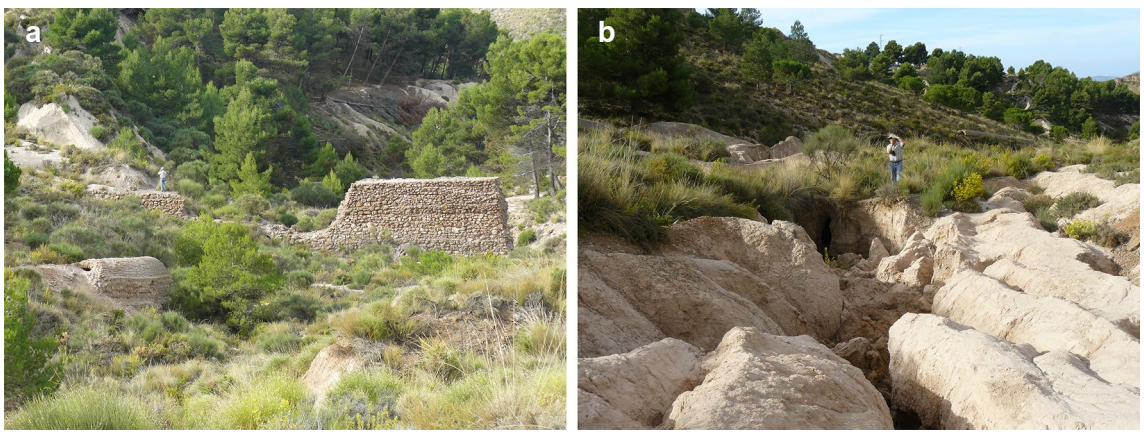

Fig. 4 **a** Breakage of the "El Segundo" mine tailings dam. **b** Aspect and thickness of mining tailings deposits next to the broken dam

soil samples were analyzed at the University of Almeria (Spain) to determine their elemental and mineralogical composition by fluorescence and x-ray diffraction (XRD), respectively (Bruker Smart Apex CCD).

Results

Soils

Two soil samples (S1 and S2) were taken in the El Segundo tailings pond (Fig. 2). X-ray diffraction showed that the main

mineral phases after all treatments to obtain F and metals such as Pb and Zn were quartz (SiO_2), calcite ($CaCO_3$), dolomite [$CaMg(CO_3)_2$], fluorite (CaF_2), and lanarkite [$Pb_2(SO_4)O$] (Table 1). The original ores of these mines were fluorite, galena, and sphalerite, with calcite, dolomite, and quartz as gangue. Lanarkite was the phase precipitated in the tailings after treatment. Similar results have been obtained in samples taken in mining tailings downstream (S3, S4, and S5). The only sample without fluorite as the mean mineral phase was collected from a nearby stream in which the flood did not flow from the tailings pond (S6).

The percentage of fluorite in these soils is high, from 16 to 40% (Table 1), with the F concentration ranging between 113 and 52 g/Kg (Table 2). The highest values were registered in the samples taken in the tailings pond, with slightly lesser values in the soils downstream. The Pb and Zn concentrations in these soils ranged between 26.4 and 7.8 g/Kg and between 15.3 and 7.7, respectively (Table 2). The concentrations in the soil sample taken in a stream not connected with the flood (S6) was 0.0, 0.15, and 0.17 g/Kg for F, Pb and Zn, respectively.

Water extracted from the soil samples indicates the relative solubility of the different elements. By studying the relationship between the concentration of different elements in these extracts and those measured in the soils, it is possible to obtain a general idea of each element's leachability. So, the average concentrations of F, Pb, and Zn in the polluted soils was compared with the mean value in the extracts. The results of these comparisons provide values of 0.28, 0.005 and 0.003 for F, Pb and Zn, respectively. These values show that F is 50 times more mobile than Pb and 80 times more than Zn.

Table 1 X-ray diffraction results for sediments

Mineral composition		%
Sample 1		
Quartz	SiO_2	28.3
Dolomite	$CaMg(CO_3)_2$	48.6
Calcite—synthetic	$Ca(CO_3)$	6.6
Fluorite, syn	CaF_2	16.5
Sample 2		
Fluorite, syn	CaF_2	27.1
Quartz	SiO_2	26.6
Silicon Oxide high quartz	SiO_2	25
Dolomite	$CaMg(CO_3)_2$	13
Lanarkite	$Pb_2(SO_4)O$	8.3
Sample 3		
Fluorite, syn	CaF_2	40
Quartz	SiO_2	35
Dolomite	$CaMg(CO_3)_2$	16.9
Calcite—synthetic	$Ca(CO_3)$	5.1
Lanarkite	$Pb_2(SO_4)O$	3
Sample 4		
Fluorite, syn	CaF_2	33.8
Quartz	SiO_2	18
Calcite—synthetic	$Ca(CO_3)$	9
Dolomite	$CaMg(CO_3)_2$	39.2
Sample 5		
Fluorite, syn	CaF_2	30.1
Quartz	SiO_2	28.5
Dolomite	$CaMg(CO_3)_2$	23.3
Lanarkite	$Pb_2(SO_4)O$	7.9
Calcite—synthetic	$Ca(CO_3)$	10.1
Sample 6		
Quartz	SiO_2	75
Dolomite	$CaMg(CO_3)_2$	16.4
Calcite—synthetic	$Ca(CO_3)$	8.6

Groundwater

Forty-one groundwater samples spread were collected over an area of 120 km^2 to determine whether the ore tailings failure affected the chemical composition of the aquifer. The samples were plotted in a modified Durov-diagram (Al-Bassam et al. 1997; Al-Bassam and Khalil 2012) and three groups of samples (G-1–G-3) can be distinguished, based on their major ions (Fig. 5). G-1 encompasses samples with calcium carbonate facies. Samples belonging to G-2 are also rich in carbonate, but the main cation in this group is Mg rather than Ca. Finally, G-3 samples are sulfated with Mg as the main cation, though some of these samples are richer in Ca.

In previous hydrogeological works in the region, four groups of samples were recognized (Vallejos et al. 2015, 2020; Díaz-Puga et al. 2016), three of which match the G-1, G-2 and G-3 groups. The forth includes Na-Cl samples related to marine intrusion. Due to the distance to the coast, samples belonging to this group do not appear in the study area.

The concentrations of F in the groundwater range from 4.3 to 0.1 ppm. The highest value was measured in a spring near the El Segundo mine, having evidently been affected by the mining activity. This is a perched spring out of the regional aquifer system. Concentrations of Zn in groundwater are an order of magnitude greater than those of Pb (Table 3).

Discussion

In the past, F, Pb and Zn ore were extracted in the study area and the resulting tailings were enriched with these elements. The principal component analysis (PCA) demonstrates that

Table 2 Results of chemical analyses of sediment samples in g/Kg and aqueous soil-sediment extracts in mg/L

Sediment	g/Kg		
	F	Zn	Pb
1S	112.90	10.04	26.36
2S	78.30	12.77	15.60
3S	80.30	13.26	10.95
4S	60.40	15.34	7.80
5S	51.50	7.71	8.73
6S	0.00	0.17	0.15
Extract sediment	mg/L		
	F	Zn	Pb
1ES	26.25	0.027	0.046
2ES	26.74	0.017	0.024
3ES	23.19	0.071	0.168
4ES	36.79	0.031	0.079
5ES	25.54	0.015	0.055
6ES	17.02	0.101	0.142
7ES	6.26	0.029	0.042
8ES	6.86	0.024	0.041

Location of sampling points in Fig. 2

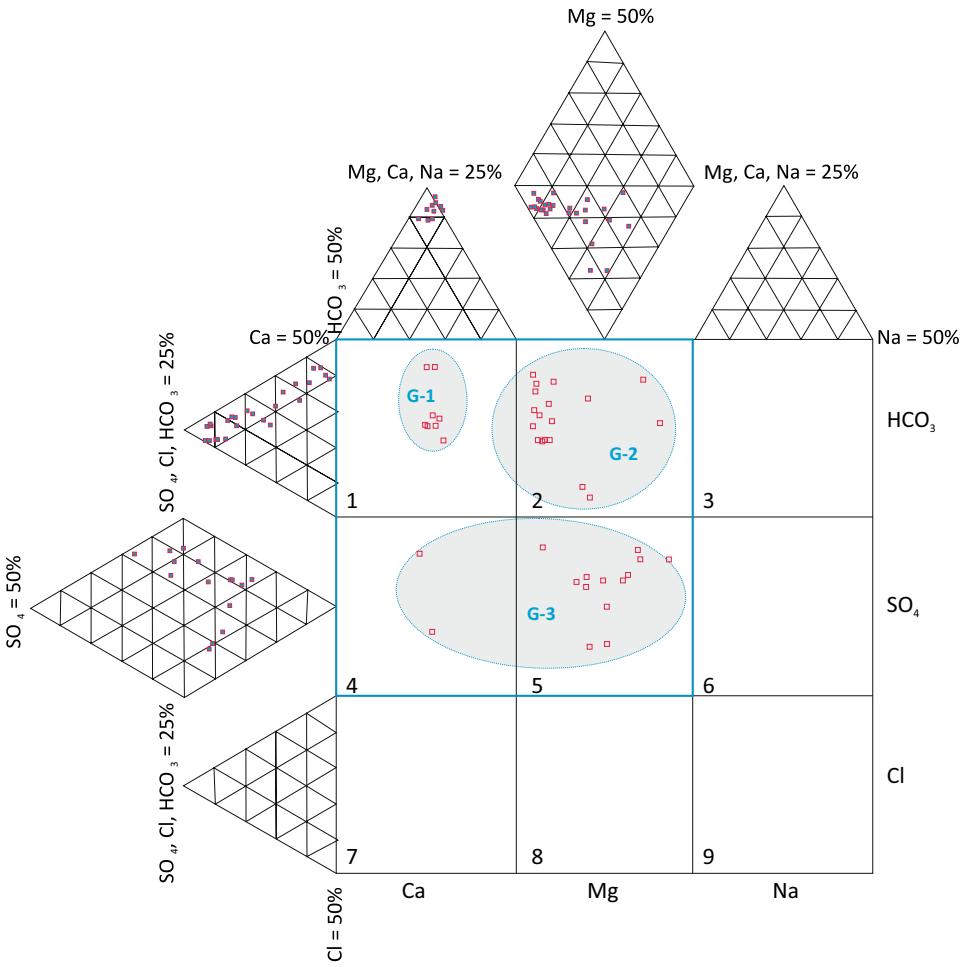

Fig. 5 Expanded Durov diagram corresponding to groundwater samples

these variables are interrelated. In this case, comparisons were made between the concentrations of the main chemical elements present in soils from ore tailings, water extracts from these soils, and the chemical composition of groundwater (Fig. 6).

The distribution of variables in the PCA of the mining soils shows that Ca and Mg concentrations tend to follow the same trend, which is logical considering that the mineralization is in dolomite rock [$CaMg(CO_3)_2$]. Other elements, such as F, are closer to metals like Pb or Zn, the other two

Table 3 Results of chemical analyses of groundwater samples in ppm

Sample	T (ºC)	EC (µS/cm)	pH	Ca	Mg	Na	K	Cl	SO_4	HCO_3	NO_3	Zn	Pb	F
1	20.8	570	7.33	63.2	37.4	12.2	1.4	14.0	96.3	274.5	24.6	0.0225	0.0005	0.533
2	17.5	315	7.93	36.9	19.9	2.2	5.9	10.0	10.7	225.7	4.4	0.0715	0.0030	0.085
3	23.2	2560	7.74	248.4	80.2	211.4	8.9	394.0	579.3	305.0	5.0	0.0390	0.0007	0.280
4	22.1	1148	7.06	97.1	63.5	71.1	4.0	100.0	211.1	298.9	33.8	0.0121	0.0004	1.815
5	19.0	724	6.89	89.9	48.0	10.1	2.3	11.0	170.5	347.7	21.9	0.0540	0.0024	1.555
6	18.6	248	8.42	21.5	18.7	4.2	0.7	8.0	6.2	143.4	7.5	0.0149	0.0005	0.033
7	19.6	946	7.66	138.9	57.9	3.1	1.2	3.0	368.2	219.6	0.1	0.0195	0.0005	2.425
8	17.5	493	7.62	72.7	34.4	3.2	0.7	4.0	142.0	231.8	4.6	0.0271	0.0056	1.425
9	17.2	555	7.35	72.0	35.2	5.8	0.9	7.0	115.4	250.1	5.2	0.0368	0.0054	1.465
10	20.4	988	7.12	109.7	64.8	29.1	6.1	29.0	228.2	372.1	47.4	0.0367	0.0008	1.355
11	18.3	775	7.28	91.6	48.3	13.1	3.0	22.0	160.2	347.7	37.7	0.1252	0.0006	1.665
12	22.4	1580	7.50	82.9	114.0	128.2	3.8	161.0	231.0	439.2	1.0	0.0170	0.0005	0.762
13	34.0	2730	7.60	258.5	93.9	282.8	11.7	398.0	588.0	335.5	1.0	0.0390	0.0005	1.625
14	21.6	1223	6.98	94.7	70.4	66.0	5.1	128.0	204.6	323.3	52.9	0.0559	0.0005	1.885
15	17.8	547	7.88	74.5	40.0	4.6	0.9	5.0	138.0	225.7	1.0	0.0130	0.0005	2.235
16	15.0	302	7.64	35.1	19.9	1.7	0.4	5.0	12.1	201.3	3.3	0.0884	0.0005	0.210
17	21.3	1141	7.76	83.9	65.9	92.0	3.8	134.0	213.0	237.9	8.0	0.0160	0.0005	2.335
18	20.5	471	7.79	54.6	33.9	14.3	1.4	15.0	66.0	274.5	4.0	0.0190	0.0005	0.238
19	20.5	553	7.92	60.1	37.4	17.9	1.6	23.0	84.0	274.5	6.0	0.0310	0.0010	0.208
20	19.0	1134	7.37	149.3	90.0	25.3	2.8	27.0	300.0	433.1	19.0	0.0150	0.0005	0.707
21	18.1	2210	6.99	212.1	189.5	345.0	8.2	112.0	666.9	481.9	207.0	0.0243	0.0006	1.355
22	20.8	1728	6.90	183.9	140.0	42.9	2.9	65.0	537.2	451.4	104.6	0.0243	0.0004	1.205
23	17.8	613	8.04	66.9	36.5	14.3	0.9	21.0	127.3	231.8	12.0	0.1644	0.0044	1.355
24	20.9	1432	7.37	144.6	127.2	19.4	4.6	34.0	462.4	402.6	64.5	0.0361	0.0013	1.635
25	7.9	281	7.90	37.7	16.0	1.5	2.6	3.0	15.7	183.0	9.9	0.0566	0.0260	4.285
26	13.7	349	7.85	37.6	23.8	4.2	0.4	6.0	65.5	176.9	6.5	0.0146	0.0007	0.551
27	17.3	382	7.69	44.4	24.5	7.3	0.7	8.0	44.0	225.7	6.7	0.0503	0.0012	1.245
28	16.3	372	8.06	44.1	23.8	7.9	0.5	7.0	34.8	237.9	7.8	0.0273	0.0004	0.955
29	22.5	1655	7.35	142.5	144.9	73.4	11.4	86.0	429.0	463.6	14.0	0.1740	0.0540	1.685
30	21.6	960	7.94	64.6	55.8	63.9	4.3	91.0	186.0	262.3	4.0	0.0090	0.0005	0.382
31	22.4	1427	7.10	131.2	88.6	76.5	3.7	121.0	338.7	353.8	25.5	0.0970	0.0022	1.945
32	17.0	535	7.49	72.4	34.5	3.1	0.7	4.0	140.5	219.6	4.0	0.0301	0.0070	1.435
33	16.1	464	7.70	56.7	29.3	2.9	1.4	8.0	102.6	231.8	5.5	0.0565	0.0002	0.615
34	19.6	975	7.12	115.0	59.8	16.2	2.1	24.0	252.0	366.0	8.0	0.0092	0.0003	0.950
35	19.7	1269	7.29	142.8	83.6	32.0	2.9	38.0	375.0	378.2	11.0	0.0808	0.0003	1.540
36	19.9	980	7.43	106.7	58.9	23.2	4.8	26.0	237.0	353.8	9.0	0.1052	0.0004	1.650
37	20.4	938	7.33	99.2	54.3	24.1	6.4	29.0	213.0	353.8	9.0	0.0591	0.0006	1.370
38	20.5	329	7.83	30.2	21.5	7.8	1.0	9.0	21.0	213.5	1.0	0.0191	0.0007	0.095
39	20.7	503	7.82	37.4	31.9	26.7	1.1	16.0	36.0	244.0	6.0	0.0157	0.0002	0.171
40	17.6	847	7.19	73.8	63.4	33.6	1.9	43.0	118.2	420.9	4.8	0.0199	0.0005	0.894
41	23.9	2020	7.03	178.5	79.9	14.8	7.9	289.0	410.2	323.3	12.2	0.0293	0.0004	1.616

Location of sampling points in Fig. 2

EC electrical conductivity

ores mined in this area (Fig. 6a). As for the PCA of the water extracted from the soils, the variables were redistributed; elements more easily dissolved were closer to each other than those that are less mobile. In this case, F is far from elements like Pb or Zn and is closer to soluble elements like Cl or Na (Fig. 6b). Finally, the PCA for the groundwater in the area affected by the tailings flood reveals that the major elements in the water were closely grouped. The minor elements, which may have acted as contaminants in certain parts of the aquifer (i.e. F, Pb and Zn), are also grouped, yet a certain distance from the major ions (Fig. 6c).

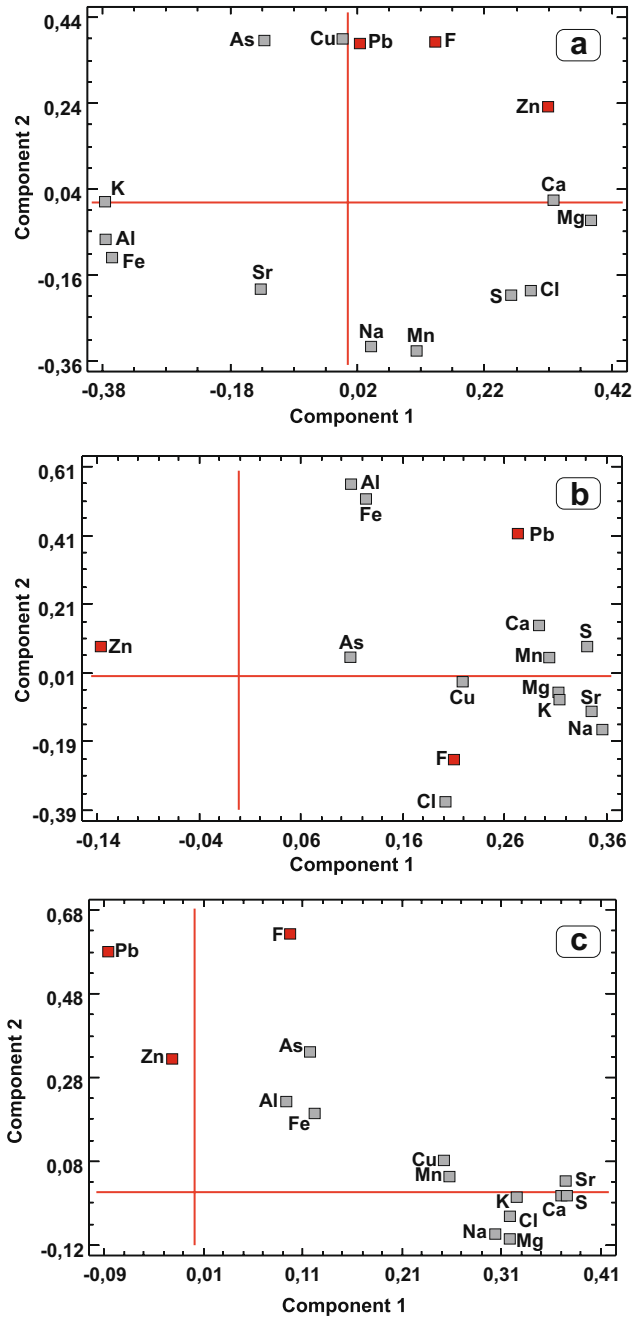

Fig. 6 Principal component analysis (PCA) plot of variables deduced from **a** sediment, **b** water extracts of sediment, **c** groundwater

With the aim of determining whether these trace elements follow some type of spatial pattern, perhaps due to the flooding event in 1966, a series of distribution maps were made that display the concentrations of certain elements in the groundwater in the study area (Fig. 7). The distribution of F on this map shows a contaminant plume surrounding the riverbed along which the tailings flowed and where they were deposited (Fig. 7). The highest values slightly surpassed the maximum value recommended by the WHO for drinking water, set at 1.5 ppm. This is significant, because some people in the area depend on this groundwater for drinking water. Areas further from the potential infiltration and contamination areas display values between 0.03 and 0.3 ppm, which correspond with the geogenic concentrations common in this area (Daniele et al. 2013). A similar scenario was observed for Pb concentrations. The sampling points with values over 1 ppm are distributed around the area contaminated by the flood. The lower mobility of this element, compared to F for example, caused the contaminated area—expanded by groundwater flow—to remain closer to the riverbed (Fig. 7). The distribution of Zn in the groundwater follows a less defined pattern, with the highest concentrations also located near the flooded area. The passing of the mining contaminants from the flood's sediment deposits to groundwater depends on both the mobility of these elements and the proximity of these sediments to the water table. One way of determining whether a contaminant is capable of reaching groundwater is by observing nitrate concentrations.

Nitrate ions can enter an aquifer through the soil via infiltration, and relatively high amounts of this component are usually linked to anthropic activity (Almasri 2007; Oren et al. 2004; Spalding and Exner 1995). Agricultural activity has been the main production sector in the study area in recent decades. Therefore, the nitrate ion can be used as an indicator of areas susceptible to contamination, to identify the possible existence of connections between superficial and deep aquifers (Pulido-Bosch et al. 2000, 2018). Figure 7 displays the sampling points with NO_3 concentrations over 10 ppm, points at which the anthropic activity of the last 50 years has reached the water table. These points are concentrated in the Berja Valley, where agricultural activity is located. The area with the highest concentration of F and Pb partially coincides with the points with high NO_3 content, meaning these elements also may have reached the saturated layer from the surface.

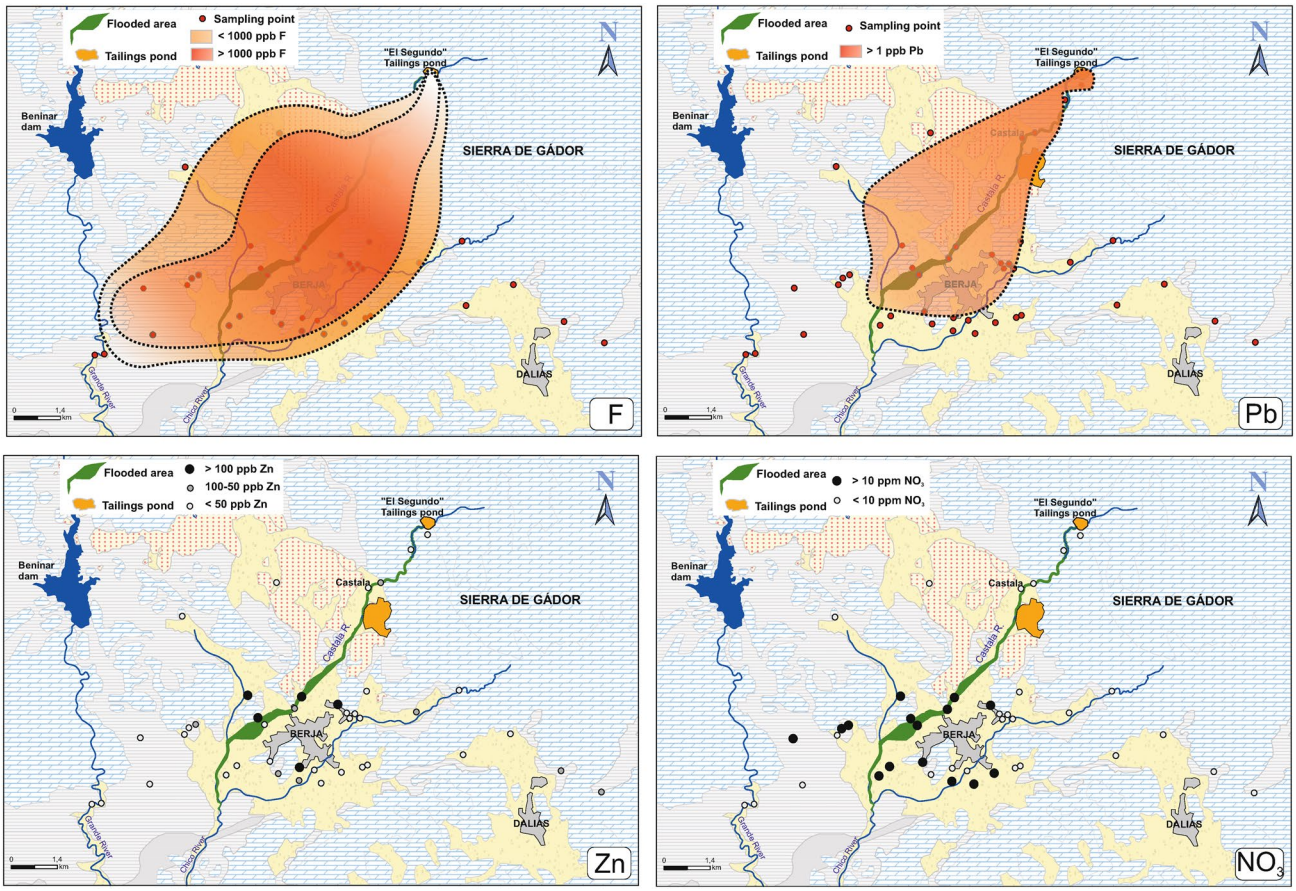

Fig. 7 Areal concentration distributions of ions in groundwater

Conclusion

More than 50 years ago, the containment dam of a pond containing mining tailings rich in F, Pb and Zn broke in the Berja area. Subsequently, the infiltration of rainwater in the deposited sediments contaminated the subjacent carbonated aquifer. At present, the F concentrations in the groundwater of the affected areas are close to 1 ppm, which surpasses the normal geogenic levels; in some cases, F concentrations exceed the maximum value recommended by the WHO for drinking water. Less mobile elements, such as Pb and Zn, also display higher concentrations in the area affected by the flood, but, not significantly, compared to the geogenic values. Portions of the tailings remain exposed in the old ponds and are susceptible to erosion and infiltration, effectively constituting a potential source of contamination for groundwater.

References

Al-Bassam AM, Khalil AR (2012) DurovPwin: a new version to plot the expanded Durov diagram for hydro-chemical data analysis. Comput Geosci 42:1–6

Al-Bassam AM, Awad HS, Al-Alawi JA (1997) DurovPlot a computer program for processing and plotting hydro-chemical data. Groundwater 35(2):362–367

Almasri MN (2007) Nitrate contamination of groundwater: a conceptual management framework. Environ Impact Asses 27:220–242

Apambire WB, Boyle DR, Michel FA (1997) Geochemistry, genesis, and health implications of fluoriferous groundwaters in the upper regions of Ghana. Environ Geol 33:13–24

Daniele L, Corbella M, Vallejos A, Díaz-Puga M, Pulido-Bosch A (2013) Geochemical simulations to assess the fluorine origin in Sierra de Gádor groundwater (SE Spain). Geofluids 13:194–203

Darrel KN, Everett AJ (1977) Fluorite solubility equilibria in selected geothermal waters. Geochim Cosmochim Acta 41:175–188

Díaz-Puga MA, Vallejos A, Sola F, Daniele L, Molina L, Pulido-Bosch A (2016) Groundwater flow and residence time in a karst aquifer using ion and isotope characterization. Int J Environ Sci Technol 13:2579–2596

Edmunds M, Smedley P (2005) Fluoride in natural waters. In: Selinus O (ed) Essentials of medical geology. Elsevier, Amsterdam, pp 301–329

Fantong WY, Satake H, Ayonghe SN, Suh EC, Adelana SMA, Fantong F, Banseka HS, Woincham W, Uehara Y, Zhang J (2010)

Geochemical provenance and spatial distribution of fluoride in groundwater of Mayo Tsanaga River Basin, far north region, Cameroon: implications for incidence of fluorosisand optimal consumption dose. Environ Geochem Hlth 32:147–163

Fawell J, Bailey K, Chilton J, Dahi E, Fewtrell L, Magara Y (2006) Fluoride in drinking-water. IWA Publ, London

Fenoll P (1987) Los yacimientos de fluorita, plomo, cinc y bario del sector central de la Cordillera Bética. PhD thesis, Universidad de Granada, Spain [in Spanish]

Gosselin DC, Headrick J, Harvey FE, Tremblay R, McFarland K (1999) Fluoride in Nebraska's ground water. Ground Water Monit Remediat 19(2):87–95

Hatje V, Pedreira RMA, De Rezende CE, França Schettini CA, de Souza GC, Marin DC, Hackspacher PC (2017) The environmental impacts of one of the largest tailing dam failures worldwide. Sci Rep-UK 7:10706

IGME (Instituto Geológico y Minero de España) (2002) Mapa metalogenético de España. Hoja 84/85. Almería-Garrucha, 1:200.000

Jacks G, Bhattachary P, Chaudhary V, Singh KP (2005) Controls on the genesis of some high-fluoride groundwaters in India. Appl Geochem 20:221–228

Kim K, Jeong GY (2005) Factors influencing natural occurrence of fluoride-rich groundwaters: a case study in the southeastern part of the Korean Peninsula. Chemosphere 58:1399–1408

Kowalski F (1999) Fluoridation. J AWWA 91:4

Macías JL, Corona-Chávez P, Sánchez-Núñez JM, Martínez-Medina M, Garduño-Monroy VH, García-Tenorio F, Cisneros-Máximo G (2015) The 27 May 1937 catastrophic flow failure of gold tailings at Tlalpujahua, Michoacán, Mexico. Nat Hazard Earth Sys 15:1069–1085

Martin JM, Braga JC (1987) Alpujárride carbonate deposits (southern Spain)—marine sedimentation in a Triassic Atlanti. Palaeogeogr Palaeocl 59:243–260

Martin JM, Torres-Ruiz J, Fontboté L (1987) Facies control of stratabound ore deposits in carbonate rocks: the F-(Pb-Zn) deposits in the Alpine Triassic of the Alpujárrides, southern Spain. Miner Deposita 22:216–226

Martín-Rojas I, Estevez A, Delgado F (2007) Unidades tectónicas y estructura general de la Sierra de Gádor y zonas adyacentes (Cordillera Bética, provincia de Almería) implicaciones paleogeográficas. Estud Geol-Madrid 63:27–42

Murray JJ (1986) Appropriate use of fluorides for human health. World Health Organization, Geneva

Oren O, Yechieli Y, Böhlke JK, Dody A (2004) Contamination of groundwater under cultivated fields in an arid environment, central Arava Valley, Israel. J Hydrol 290:312–328

Owen JR, Kemp D, Lèbre E, Svobodova K, Pérez Murillo G (2020) Catastrophic tailings dam failures and disaster risk disclosure. Int J Disast Risk Re 42:101361

Pulido-Bosch A, Bensi S, Molina L, Vallejos A, Calaforra JM, Pulido-Leboeuf P (2000) Nitrates as indicators of aquifer interconnection Application to the Campo de Dalías (SE–Spain). Environ Geol 39(7):791–799

Pulido-Bosch A, Rigol-Sánchez JP, Vallejos A, Andreu JM, Cerón JC, Molina-Sanchez L, Sola F (2018) Impacts of agricultural irrigation on groundwater salinity. Environ Earth Sci 77:197

Queiroz HM, Nóbrega GN, Ferreira TO, Almeida LS, Romero TB, Santaella ST, Bernardino AF, Otero XL (2018) The Samarco mine tailing disaster: a possible time-bomb for heavy metals contamination? Sci Total Environ 637–638:498–506

Resongles E, Casiot C, Freydier R, Dezileau L, Viers J, Elbaz-Poulichet F (2014) Persisting impact of historical mining activity to metal (Pb, Zn, Cd, Tl, Hg) and metalloid (As, Sb) enrichment in sediments of the Gardon River, southern France. Sci Total Environ 481:509–521

Rukah YA, Alsokhny K (2004) Geochemical assessment of groundwater contamination with special emphasis on fluoride concentration, north Jordan. Chem Erde-Geochem 64:171–181

Spalding RF, Exner ME (1995) Occurrence of nitrate in groundwater—a review. J Environ Qual 22:392–402

Thompson F, de Oliveira BC, Cordeiro MC, Masi BP, Rangel TP, Paz P, Freitas T, Lopes G, Silv BS, Cabral SA, Soares M, Lacerda D, dos Santos C, Lopes-Ferreira M, Lima C, Thompson C, de Rezende CE (2020) Severe impacts of the Brumadinho dam failure (Minas Gerais, Brazil) on the water quality of the Paraopeba River. Sci Total Environ 705:135914

Vallejos A, Díaz-Puga MA, Sola F, Daniele L, Pulido-Bosch A (2015) Using ion and isotope characterization to delimitate a hydrogeological macrosystem. Sierra de Gádor (SE, Spain). J Geochem Explor 155:14–25

Vallejos A, Daniele L, Sola F, Molina L, Pulido-Bosch A (2020) Anthropic-induced salinization in a dolomite coastal aquifer Hydrogeochemical processes. J Geochem Explor 209:106438

Vithanage M, Bhattacharya P (2015) Fluoride in the environment: sources, distribution and defluoridation. Environ Chem Lett 13:131–147

WHO (2017) Guidelines for drinking water quality. World Health Organization, Geneva